proceedings

MDPI

Proceedings

Design of a Quasi-Direct-Drive Actuator for Dynamic Motions †

Akash Singh [1,2,*,‡], Navvab Kashiri [1] and Nikolaos Tsagarakis [1]

[1] Istituto Italiano di Tecnologia, 16163 Genova GE, Italy; Navvab.Kashiri@iit.it (N.K.); nikos.tsagarakis@iit.it (N.T.)
[2] Dipartimento di Informatica, Bioingegneria, Robotica e Ingegneria dei Sistemi, University of Genoa, 16145 Genova GE, Italy
* Correspondence: Akash.singh@iit.it; Tel.: +39-366-343-0855
† Presented at the First International Electronic Conference on Actuator Technology: Materials, Devices and Applications, 23–27 November 2020; Available online: https://iecat2020.sciforum.net/.
‡ Current address: Via S. Quirico 19d, 16163 Genova, Italy.

Published: 21 November 2020

Abstract: In recent years, several legged/wheeled robots have been developed, and their effective functionality in locomotion on uneven terrains has been proved. Many robotics researchers have been focusing on improving the locomotion speed as well as the stability and robustness of such robots. High-speed locomotion of robots is, however, subject to various design challenges, especially in the development of actuators. The robotic applications that require high-speed motion in high-torque operations along with the ability to manage dynamic physical interactions are not satisfied by the conventional robotic actuators deploying high-reduction gearings. In this work, we present a quasi-direct-drive actuator designed for continuous high-speed motions in high torque, such as wheeled motions in mobile robots or joint motions in dynamic-legged robots. The presented actuator exploits low-reduction gearing so that it can render over 26 Nm of continuous torque, while the actuator speed can exceed 37 rad/s. Such characteristics enable the exhibition of dynamic motions and can deal with large external impacts. The selection of the motor and design of the gearing unit was carried out iteratively so that commercial items with minimum customization could be employed and the outer diameters of the motor and the gearbox could match. A single-level planetary gearbox was devised for the reduction unit to ensure high back-drivability and transparency of the actuator, thereby making the actuator robust against external impacts and allowing for accurate torque control using motor current measurement. The gear set design was carried out based on the AGMA gear torque calculation. Given the radial space required for the gearbox to deal with the torque requirements, the actuator motor was chosen to be small in height (pancake type), which ensures high torque density within smaller dimensions at high-speed operation. The mechanical design of the actuator is presented in this paper, and the actuator's specifications in terms of size and performance are compared with those of similar state-of-the-art actuators.

Keywords: actuator; direct drive; back-drivable

1. Introduction

The development of legged/wheeled robots has allowed the exploration of external environments for applications such as urban search and rescue. Such applications often include maneuvers in rough and uneven terrains that are subject to unexpected interactions and abrupt impacts. To account for different performance criteria, including mechanical resilience and energy efficiency, the development of robotic actuators introduces problems [1]. Conventional geared actuators that are also commercially

available have managed to provide high torque density and control bandwidth, but only at the cost of significant friction and increased reflected inertia. While strain-wave gearing solutions (e.g., harmonic drives that significantly reduce the actuator mass and the friction) improve the torque density and enable back-drivability, they present unwanted flexibility and are vulnerable to external impacts.

A set of state-of-the-art actuators, known as series elastic actuators (SEAs; see, e.g., [2–4]), have to compromise bandwidth to obtain compliance, enabling harsh and/or unwanted interactions, in addition to other advantages, such as energy efficiency in resonance motions. Several variations of SEAs have been developed to permit the control of the intrinsic stiffness (see, e.g., [5]) and damping (see, e.g., [6]), or to grant the replication of user-designed nonlinear stiffness and damping profiles (see, e.g., [7]). Despite the benefits introduced by the intrinsic compliance, these actuators integrate additional components that increase the system complexity and mass, thereby resulting in limited benefits, especially for dynamic locomotion. Direct-drive actuators [8,9], on the other hand, do not use gear reduction, thus eliminating the problems associated with gearboxes. They introduce high force transparency and are mechanically robust. However, most of these actuators are unable to provide a sufficiently large torque for common robotics applications when mass limitations are taken into account.

To address the limitations of direct-drive units and high-reduction geared actuators, quasi-direct-drives have been developed to generate sufficiently large torques required for a given application without sacrificing back-drivability and/or mechanical resilience. These drives are often composed of torque motors (in contrast to power/speed motors) and a single-stage gearing transmission, so that the output torque is amplified to some extent and intrinsic back-drivability is achieved without compromising the system bandwidth. Moreover, while torque sensors (such as [10]) are an essential part of state-of-the-art robotic platform actuators (e.g., [11]), the low reduction of the gearing and the resulting high efficiency allows the motor torque, which can be realized by the current measurement, to directly be a valid indication of the output torque. Such a design provides an actuation solution for robots rendering dynamic motions, such as jumping, as presented in the MIT cheetah robot [12–14]. A similar customized quasi-direct-drive actuator was developed for the mini cheetah robot [15], which operates at lower torques. Yu et al. [16] presented the BIRO(Biomechatronics and Intelligent Robotics) actuator based on a high-torque-density customized motor to develop a quasi-direct-drive for an exoskeleton with a peak torque of 42 Nm; however, the maximum speed it can reach is about 19 rad/s. The Stanford Doggo [17], a light-weight jumping robot, uses an out-runner motor with a fairly low reduction to render considerably fast motion at the cost of low torque. Table 2 details the available specifications of these actuators as compared to that of the proposed actuator.

This work introduces an actuator design for a new legged/wheeled hybrid robot that is specifically targeted to perform fast and explosive motions while also being capable of supporting heavy-load applications. The article presents the details of the mechanical design of the actuator, which relies upon commercial/datasheet components, therefore limiting the customization and fabrication of mechanical parts to the corresponding housing and support parts, so that we can achieve a more economical, yet reliable, solution, which is tailored to the requirements of our target platform.

2. Actuator Design

The selection of components was carried out through an iterative process on the basis of the minimum torque and speed requirements determined from the specifications of the target platform, while we designed the gearbox to include only one-stage reduction. The target continuous and peak output torques of the actuator are 20 and 40 Nm, respectively, and the target no-load speed is selected as 20 rad/s. The motor and gearbox selection was, therefore, carried out in such a way that the outer diameters of the motor and the gearbox were as close as possible to each other so that the outer envelope of the actuator could be fairly continuous. The selected frameless motor is the Tecnotion QTR 105-25Z, which is a flat (pancake type) motor that can generate 3.3 Nm of continuous torque, while its peak torque can reach up to 6.9 Nm, and its speed can exceed 2700 rpm. It generates the target torques

with a reduction ratio of 8:1, even when a fairly conservative overall efficiency of 80% is accounted for, while the no-load speed will be significantly higher than the target maximum speed.

The actuator assembly is shown in Figure 1, and consists two sub-assemblies: the motor and the gearbox. The motor sub-assembly is shown on the left, and consists of the frameless motor and the corresponding parts, including the stator housing, and the rotor shaft on which the gearbox input pinion is also assembled. The gearbox sub-assembly is shown in the middle of Figure 1, and includes the planet gears and their supporting carrier, as well as the ring gear. The gears are made of steel molybdenum alloy material produced by Kyouiku Gears. Table 1 details the specifications of the selected gears, including the torque rating. The maximum tooth strength of the gears was studied, and the AGMA(The American Gear Manufacturers Association) gear torque calculation formula [18] was used to ensure correct selection of the thickness, module, and material of the gears. Considering shape, geometry, and load factors specific to the gears, the maximum strength of the gear teeth and the corresponding torque per tooth T_g were calculated by Equations (1) and (2), respectively:

$$W_t = \sigma K_v J m F / K_m, \tag{1}$$

$$T_g = P_d W_t / 2, \tag{2}$$

where W_t symbolizes the maximum shear strength of the gear teeth, σ is the allowable tooth root bending stress, K_v and J are the dynamic and geometry factors of the teeth, m is the gear tooth module, F is the face width, K_m is the load distribution factor, and P_d is the pitch diameter of the gear.

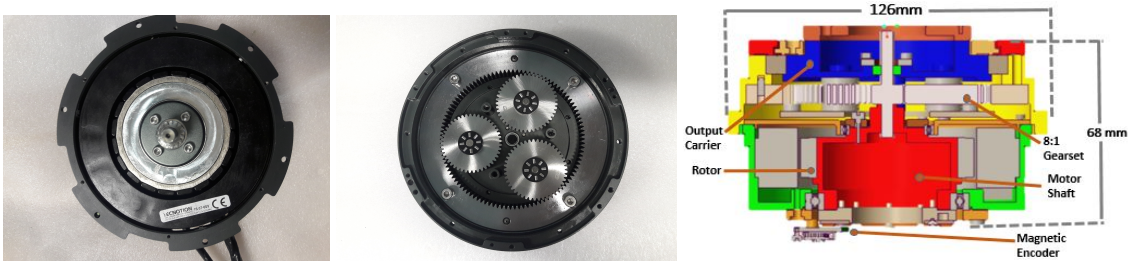

(**a**) (**b**) (**c**)

Figure 1. Figures from left: (**a**) the motor sub-assembly; (**b**) the gearbox sub-assembly; (**c**) the cross-sectional view of the actuator assembly in CAD, fitting into dimensions of 126 × 68 mm.

An important step in planetary gear design is to specify the number of planet gears. While increasing the number of planet gears reduces the load per tooth, the maximum number of planet gears is often limited by space and geometry. Moreover, the addition of planet gears also escalates the overall cost and noise, and it is therefore desired to employ the minimum number of planet gears required to mesh with the pinion gear (sun), which is attached to the motor shaft to support the ultimate stall torque of the motor. Table 1 also reports the maximum torque that can be transferred through the gears per tooth when utilizing three planet gears, as compared to the maximum admissible torque on the basis of the gear tooth shear strength extracted from (1). The maximum torque that can be applied to the pinion is set based on the ultimate torque of the motor, which leads to $\frac{6.9}{3} = 2.3$ Nm torque per tooth when using three planet gears, while the torques applied to the planet and ring gears are derived using a static analysis of the gears.

Table 1. Maximum torque that can be provided by the gears.

Gears	Number of Teeth	Pitch Diameter	Module	Load Dist. Factor	Dynamic Factor	Geometry Factor	Max Admissible Torque per Tooth	Max Torque Applied per Tooth
Pinion	15	12	0.8	1.3	0.75	0.29	2.34	2.3
Planets	45	36	0.8	1.3	0.74	0.35	8.49	6.9
Ring	105	84	0.8	1.3	0.8	0.42	17.36	16.1

The total weight of the proposed actuator is about 1.9 Kg, and generates continuous and peak output torques of about 26.4 and 55.2 Nm without accounting for losses. The maximum speed reaches 37.2 rad/s with a 48 V bus voltage when only quadrature axis current is applied, while the implementation of field-weakening controllers can boost the maximum velocity (see, e.g., [19,20]). To this end, the rotor motion was measured using a 19-bit AkSim magnetic encoder, thereby allowing for straightforward field-oriented current control. The lower-level controller was implemented on custom electronics, where the innermost current loop was executed at 20 kHz, and the outer velocity loop was run at 2 kHz. The communication of the higher-level interface and the lower level was carried out through the EtherCAT communication protocol.

Table 2 presents comparisons of some of the state-of-the-art quasi-direct-drive actuators with the presented actuator. It shows that the proposed unit relying mainly upon commercial components (motor, gears, bearings, and other critical components) can exhibit notable characteristics. To present a quantifiable comparison, we defined an index based on the peak torque density and maximum reachable speed. By comparing the two drives proposed by the MIT group, we can see that this power-density-like index drops by about six times when the peak torque increases by around three times. This shows that our proposed unit renders an index about five times that of the MIT cheetah while generating a fairly similar peak torque, and renders a fairly higher power-density-like index than the BIRO actuator, while the proposed drive can generate 50% higher peak torque.

Table 2. The specifications of the proposed actuators as compared to state-of-the-art quasi-direct drives.

Actuator	Dimensions (mm)	Peak Torque (Nm)	Nominal Torque (Nm)	Maximum Speed (rad/s)	Peak Torque Density × Maximum Speed (W/kg)	Weight (Kg)
MIT Cheetah 1	N/A	58	N/A	6.9 *	219.29	1.825
Mini Cheetah	96×40	17	6.9	40	1360	0.5
BIRO	110×51	36	17.1	19	876.9	0.78
Stanford Doggo	N/A	4.8	1.51	251	3675	0.28
Proposed actuator	126×68	55.2	26.4	37.2	1086.47	1.89

* The value was computed using the corresponding motor torque constant of 0.4 Nm/A and the supply voltage of 100 V, and considering the reduction ratio of 1:5.8, as reported in [12].

3. Experimental Results

To validate the performance of the actuator, specifically in terms of peak speed and continuous torque, two experiments were performed when the drive was velocity controlled:

1. Nominal Torque Evaluation: The actuator output shaft was attached to a lever with a set of loads weighing about 14 Kg hanging at a 20 cm distance with respect to the joint axis, replicating an external torque of approximately 28 Nm, which is slightly higher than the continuous torque of the actuator. A set of velocity references was commanded until the lever reached the horizontal position, and it was held in that condition. The time history of the current associated with this test is shown in Figure 2.

2. Maximum Speed Evaluation: The actuator output was free, and a few direct current commands were set to render the maximum velocity with the actuator, which was about 37 rad/s when taking about 4 A to overcome the frictional and other losses. The corresponding time history of the current and velocity is illustrated in Figure 3.

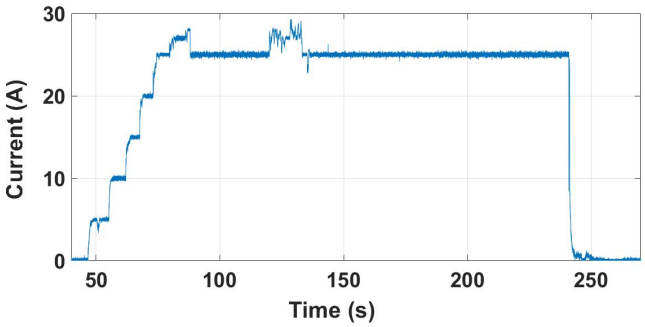

Figure 2. Time history of the current when executing a torque of 28 Nm.

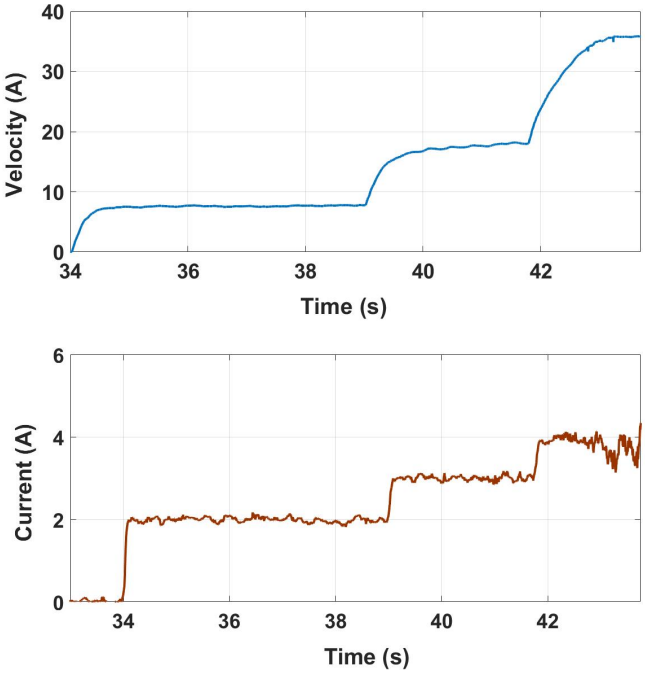

Figure 3. Time history of the current and velocity when moving with no load.

4. Conclusions

This article introduces the design of a new quasi-direct-drive actuator on the basis of a high-torque-density motor and a low-reduction-ratio gearing transmission. The proposed design was discussed, and the actuator was successfully developed. The experimental results validate the target characteristics of the actuator in terms of torque and speed, and they present the potential of the proposed drive for powering a platform that can perform dynamic motions and can exhibit high strength.

References

1. Kashiri, N.; Abate, A.; Abram, S.J.; Albu-Schaffer, A.; Clary, P.J.; Daley, M.; Faraji, S.; Furnemont, R.; Garabini, M.; Geyer, H.; et al. An overview on principles for energy efficient robot locomotion. *Front. Robot. AI* **2018**, *5*, 129.
2. Pratt, G.A.; Williamson, M.M. Series elastic actuators. In Proceedings of the IEEE/RSJ International Conference on Intelligent Robots and Systems, Pittsburgh, PA, USA, 5–9 August 1995; Volume 1, pp. 399–406.
3. Tsagarakis, N.G.; Laffranchi, M.; Vanderborght, B.; Caldwell, D.G. A compact soft actuator unit for small scale human friendly robots. In Proceedings of the IEEE international Conference on Robotics and Automation, Kobe, Japan, 12–17 May 2009; pp. 4356–4362.
4. Hutter, M.; Remy, C.D.; Hoepflinger, M.A.; Siegwart, R. Scarleth: Design and control of a planar running robot. In Proceedings of the IEEE/RSJ International Conference on Intelligent Robots and Systems, San Francisco, CA, USA, 25–30 September 2011; pp. 562–567.
5. Grioli, G.; Wolf, S.; Garabini, M.; Catalano, M.; Burdet, E.; Caldwell, D.; Carloni, R.; Friedl, W.; Grebenstein, M.; Laffranchi, M.; et al. Variable stiffness actuators: The user's point of view. *Int. J. Robot. Res.* **2015**, *34*, 727–743.
6. Laffranchi, M.; Chen, L.; Kashiri, N.; Lee, J.; Tsagarakis, N.G.; Caldwell, D.G. Development and control of a series elastic actuator equipped with a semi active friction damper for human friendly robots. *Robot. Auton. Syst.* **2014**, *62*, 1827–1836.
7. Kashiri, N.; Caldwell, D.G.; Tsagarakis, N. A self-adaptive variable impedance actuator based on intrinsic non-linear compliance and damping principles. In Proceedings of the 2017 IEEE International Conference on Robotics and Automation (ICRA), Singapore, 29 May–3 June 2017; pp. 1248–1254.
8. Asada, H.; Youcef-Toumi, K. *Direct-Drive Robots: Theory and Practice*; MIT Press: Cambridge, MA, USA, 1987.
9. Carignan, C.R.; Cleary, K.R. Closed-Loop Force Control for Haptic Simulation of Virtual Environments. 2000; pp. 1–14. Available online: https://www.researchgate.net/publication/243766717_Closed-loop_force_control_for_haptic_simulation_of_virtual_environments.
10. Kashiri, N.; Malzahn, J.; Tsagarakis, N.G. On the sensor design of torque controlled actuators: A comparison study of strain gauge and encoder-based principles. *IEEE Robot. Autom. Lett.* **2017**, *2*, 1186–1194.
11. Kashiri, N.; Baccelliere, L.; Muratore, L.; Laurenzi, A.; Ren, Z.; Hoffman, E.M.; Kamedula, M.; Rigano, G.F.; Malzahn, J.; Cordasco, S.; et al. CENTAURO: A hybrid locomotion and high power resilient manipulation platform. *IEEE Robot. Autom. Lett.* **2019**, *4*, 1595–1602.
12. Seok, S.; Wang, A.; Chuah, M.Y.; Hyun, D.J.; Lee, J.; Otten, D.M.; Lang, J.H.; Kim, S. Design principles for energy-efficient legged locomotion and implementation on the MIT cheetah robot. *IEEE/ASME Trans. Mechatronics* **2014**, *20*, 1117–1129.
13. Wensing, P.M.; Wang, A.; Seok, S.; Otten, D.; Lang, J.; Kim, S. Proprioceptive actuator design in the MIT Cheetah: Impact mitigation and high-bandwidth physical interaction for dynamic legged robots. *IEEE Trans. Robot.* **2017**, *33*, 509–522.
14. Ding, Y.; Park, H.W. Design and experimental implementation of a quasi-direct-drive leg for optimized jumping. In Proceedings of the 2017 IEEE/RSJ International Conference on Intelligent Robots and Systems (IROS), Vancouver, BC, Canada, 24–28 September 2017; pp. 300–305.
15. Katz, B.; Di Carlo, J.; Kim, S. Mini cheetah: A platform for pushing the limits of dynamic quadruped control. In Proceedings of the IEEE International Conference on Robotics and Automation, Montreal, QC, Canada, 20–24 May 2019; pp. 6295–6301.
16. Yu, S.; Huang, T.H.; Yang, X.; Jiao, C.; Yang, J.; Chen, Y.; Yi, J.; Su, H. Quasi-Direct Drive Actuation for a Lightweight Hip Exoskeleton with High Backdrivability and High Bandwidth. *IEEE/ASME Trans. Mechatronics* **2020**, *25*, 1794–1802.
17. Kau, N.; Schultz, A.; Ferrante, N.; Slade, P. Stanford doggo: An open-source, quasi-direct-drive quadruped. In Proceedings of the IEEE International Conference on Robotics and Automation, Montreal, QC, Canada, 20–24 May 2019; pp. 6309–6315.
18. Association, A.G.M.; Institute, A.N.S. *Fundamental Rating Factors and Calculation Methods for Involute Spur and Helical Gear Teeth*; AGMA Standard; American Gear Manufacturers Association: Alexandria, VA, USA, 2004.

19. Roozing, W.; Kashiri, N.; Tsagarakis, N.G. Enhanced explosive motion for torque controlled actuators through field weakening control. In Proceedings of the 2018 IEEE/RSJ International Conference on Intelligent Robots and Systems (IROS), Madrid, Spain, 1–5 October 2018; pp. 1–8.
20. Mohammadnia, M.; Kashiri, N.; Braghin, F.; Tsagarakis, N.G. Flux Regulation for Torque-controlled Robotics Actuators. In Proceedings of the 2019 19th International Conference on Advanced Robotics (ICAR), Belo Horizonte, Brazil, 2–6 December 2019; pp. 93–98.